Applied and Environmental Microbiology, May 2008, p. 2766–2777 Vol. 74, No. 9
0099-2240/08/$08.00+0 doi:10.1128/AEM.02591-07

Malic Acid Production by *Saccharomyces cerevisiae*: Engineering of Pyruvate Carboxylation, Oxaloacetate Reduction, and Malate Export[▽]†

Rintze M. Zelle,[1,4]‡ Erik de Hulster,[1,4]‡ Wouter A. van Winden,[1,4] Pieter de Waard,[3] Cor Dijkema,[3] Aaron A. Winkler,[2] Jan-Maarten A. Geertman,[1,4] Johannes P. van Dijken,[1,2,4] Jack T. Pronk,[1,4] and Antonius J. A. van Maris[1,4]*

Department of Biotechnology, Delft University of Technology, Julianalaan 67, 2628 BC Delft, The Netherlands[1]; BIRD Engineering B.V., Westfrankelandsedijk 1, 3115 HG Schiedam, The Netherlands[2]; Wageningen NMR Centre, Wageningen University and Research Centre, Dreijenlaan 3, 6703 HA Wageningen, The Netherlands[3]; and Kluyver Centre for Genomics of Industrial Fermentation, Julianalaan 67, 2628 BC Delft, The Netherlands[4]

Received 16 November 2007/Accepted 1 March 2008

Malic acid is a potential biomass-derivable "building block" for chemical synthesis. Since wild-type *Saccharomyces cerevisiae* strains produce only low levels of malate, metabolic engineering is required to achieve efficient malate production with this yeast. A promising pathway for malate production from glucose proceeds via carboxylation of pyruvate, followed by reduction of oxaloacetate to malate. This redox- and ATP-neutral, CO_2-fixing pathway has a theoretical maximum yield of 2 mol malate (mol glucose)$^{-1}$. A previously engineered glucose-tolerant, C_2-independent pyruvate decarboxylase-negative *S. cerevisiae* strain was used as the platform to evaluate the impact of individual and combined introduction of three genetic modifications: (i) overexpression of the native pyruvate carboxylase encoded by *PYC2*, (ii) high-level expression of an allele of the *MDH3* gene, of which the encoded malate dehydrogenase was retargeted to the cytosol by deletion of the C-terminal peroxisomal targeting sequence, and (iii) functional expression of the *Schizosaccharomyces pombe* malate transporter gene Sp*MAE1*. While single or double modifications improved malate production, the highest malate yields and titers were obtained with the simultaneous introduction of all three modifications. In glucose-grown batch cultures, the resulting engineered strain produced malate at titers of up to 59 g liter^{-1} at a malate yield of 0.42 mol (mol glucose)$^{-1}$. Metabolic flux analysis showed that metabolite labeling patterns observed upon nuclear magnetic resonance analyses of cultures grown on ^{13}C-labeled glucose were consistent with the envisaged nonoxidative, fermentative pathway for malate production. The engineered strains still produced substantial amounts of pyruvate, indicating that the pathway efficiency can be further improved.

Malic acid, a four-carbon dicarboxylic acid, is currently used mainly as an acidulant and taste enhancer in the beverage and food industry. Racemic malic acid is synthesized petrochemically from maleic anhydride. Enantiomerically pure L-malic acid (e.g., for production of pharmaceuticals) is produced from fumarate (synthesized from maleic anhydride) by enantioselective hydration with fumarase, using either immobilized cells or isolated enzyme (6, 19). Increasing oil prices, concerns about climate change, and advances in the field of metabolic engineering have fueled renewed interest in the production of organic acids by microbial fermentation (20). In 2004, the U.S. Department of Energy included a group of 1,4-dicarboxylic acids, consisting of succinic, fumaric, and malic acids, in the top 12 most interesting chemical building blocks that can be derived from biomass (61).

In 1924, malic acid was identified as a product of yeast fermentation (7). Since then, malic acid production has been observed for a wide range of microorganisms. Fermentative production of malic acid has been most successfully demonstrated with *Aspergillus flavus*, achieving 63% of the maximum theoretical yield of malic acid on glucose at high production rates and titers (4). Since its potential aflatoxin production disqualified *A. flavus* as a producer of food-grade chemicals (16), malic acid production was studied with other organisms, including the yeast *Saccharomyces cerevisiae* (Table 1). The highest reported malic acid concentration obtained with *S. cerevisiae* thus far is 12 g liter^{-1}, which was achieved by overexpression of the cytosolic isoenzyme of malate dehydrogenase (Mdh2p) (41). Recently, another yeast, a natural isolate of *Zygosaccharomyces rouxii*, was shown to produce up to 75 g liter^{-1} of malic acid in a complex medium containing 300 g liter^{-1} glucose (48).

Four metabolic pathways for the production of L-malic acid from glucose can be identified (Fig. 1). (i) The first of these is carboxylation of pyruvate (*S. cerevisiae* lacks phosphoenolpyruvate carboxylase) to oxaloacetate, followed by reduction of oxaloacetate to malate. If pyruvate is produced in glycolysis, this nonoxidative pathway is ATP neutral and involves a net

* Corresponding author. Mailing address: Department of Biotechnology, Delft University of Technology, Julianalaan 67, 2628 BC Delft, The Netherlands. Phone: 31 15 2782412. Fax: 31 15 2782355. E-mail: A.J.A.vanMaris@TUDelft.nl.

† Supplemental material for this article may be found at http://aem.asm.org/.

‡ R.M.Z. and E.D.H. contributed equally to this publication.

▽ Published ahead of print on 14 March 2008.

TABLE 1. Overview of production titers, yields, and rates presented in various studies of malic acid production by fermentation-based processes[a]

Organism(s)	Year	Malic acid (g liter^{-1})	Yield (mol mol^{-1})	Productivity (g liter^{-1} h^{-1})	Reference
A. flavus	1962	60	0.84	0.1	Abe et al. (1)
	1988	36	0.51	0.19	Peleg et al. (39)
	1991	113	1.26	0.59	Battat et al. (4)
Rhizopus arrhizus and *Paecilomyces varioti*	1983	48	0.81	0.34	Takao et al. (49)
Monascus araneosus	1993	28	0.50	0.23	Lumyong and Tomita (30)
Schizophyllum commune	1997	18	0.48	0.16	Kawagoe et al. (26)
Z. rouxii	2007	75	0.52	0.54	Taing and Taing (48)
S. cerevisiae	1984	1		0.01	Fatichenti et al. (12)
	1988	2			Schwartz and Radler (45)
	1996	6	0.09[b]	0.18	Pines et al. (40)
	1997	12	0.13[b]	0.38	Pines et al. (41)
	2008	59	0.42	0.19	This study

[a] Yields are given in mol malate per mol glucose unless otherwise indicated.
[b] Galactose was used as the carbon source instead of glucose.

fixation of CO_2, resulting in a maximum theoretical malate yield of 2 mol (mol glucose)$^{-1}$. (ii) The second pathway is condensation of oxaloacetate and acetyl-coenzyme A (acetyl-CoA) to citric acid, followed by its oxidation to malate via the tricarboxylic acid (TCA) cycle. If acetyl-CoA is generated by pyruvate dehydrogenase and oxaloacetate by pyruvate carboxylase, the conversion of glucose to malate via this oxidative pathway results in the release of 2 CO_2, thus limiting the maximum theoretical malate yield to 1 mol (mol glucose)$^{-1}$. (iii) Formation of malate from two molecules of acetyl-CoA via the glyoxylate cycle is the third pathway. In this alternative oxidative pathway for malate production, the maximum malate yield on glucose is limited to 1 mol mol^{-1} due to the oxidative decarboxylation reaction required for acetyl-CoA production from pyruvate. (iv) Fourth is a noncyclic pathway that involves the glyoxylate cycle enzymes, but in which oxaloacetate is replenished by pyruvate carboxylation, resulting in a theoretical maximum yield of 1 1/3 mol malate per mol glucose.

Metabolic engineering of *S. cerevisiae* for high-yield production of organic acids requires the elimination of alcoholic fermentation which, in this yeast, occurs even under fully aerobic conditions when high concentrations of sugar are present (42, 57). While deletion of the three pyruvate decarboxylase genes (*PDC1*, *PDC5*, and *PDC6*) in *S. cerevisiae* completely prevents alcoholic fermentation (24), C_2 compound auxotrophy and intolerance for high glucose levels (13, 14) complicate the use of pyruvate decarboxylase-negative (Pdc$^-$) strains as a metabolic engineering platform. In a previous study, we applied evolutionary engineering in batch and chemostat cultures to select a glucose-tolerant, C_2-independent Pdc$^-$ *S. cerevisiae* strain (53). In aerobic, glucose-grown batch cultures, this strain produced large amounts of pyruvate, which is an intermediate for malate production.

The aim of the present study is to explore a strategy for the metabolic engineering of Pdc$^-$ *S. cerevisiae* for malate production that encompasses carboxylation of pyruvate to oxaloacetate, followed by reduction to malate, a route with a maximal theoretical yield of 2 mol malate per mol of glucose. To this end, the impact on malate production of the separate and combined introduction of three genetic modifications will be analyzed in a glucose-tolerant, C_2-independent Pdc$^-$ strain: (i) overexpression of pyruvate carboxylase, (ii) high-level expression of cytosolic malate dehydrogenase activity, and (iii) functional expression of a heterologous malate transporter, because malate transport rates via diffusion across the *S. cerevisiae* plasma membrane (58) may be too low for efficient malate production. To verify whether the malate produced by an engineered strain was indeed produced via the envisaged nonoxidative pathway, metabolic flux analysis was performed, based on ^{13}C nuclear magnetic resonance (^{13}C-NMR) labeling data of extracellular metabolites after cultivation on [1-^{13}C]glucose.

MATERIALS AND METHODS

Strains and maintenance. All strains used in this study (Table 2) are derived from the *S. cerevisiae* CEN.PK strain family (51). Stock cultures were prepared from shake flask cultures by the addition of glycerol to culture broth (20% vol/vol) and storage of 2-ml aliquots in sterile vials at −80°C. Stock cultures were grown on a synthetic medium consisting of demineralized water, 20 g liter^{-1} glucose, 5 g liter^{-1} $(NH_4)_2SO_4$, 3 g liter^{-1} KH_2PO_4, 0.5 g liter^{-1} $MgSO_4 \cdot 7H_2O$, vitamins, and trace elements (56), with a pH of 6 (set with KOH). During construction, strains were maintained on complex medium (YP; 10 g liter^{-1} yeast extract and 20 g liter^{-1} peptone [both from BD Difco]) or synthetic medium (MY) (56) supplemented with glucose (2%) as the carbon source (YPD or MYD) and, for the plates, with 1.5% agar.

Construction of a *trp1* null mutant of *S. cerevisiae* TAM. All *S. cerevisiae* strains in this study are based on the *ura3*Δ Pdc$^-$ TAM strain (53). To allow for the introduction of additional plasmids, a second marker was introduced by deletion of *TRP1*. A deletion cassette that confers Geneticin resistance was made by performing a PCR on plasmid pUG6 (22) using the oligopeptides 5′trp1::kanlox and 3′trp1::kanlox (Table 3) and was used for the transformation of TAM. Transformants were selected on YPD containing 200 μg ml^{-1} Geneticin (G418; Invitrogen/GIBCO), restreaked on the same medium, and verified by testing for tryptophan auxotrophy and by diagnostic PCR, using 5′TRP1 plus KanA and 3′TRP1 plus KanB primers (Table 3). RWB961 was identified as a *trp1* deletion mutant and was used to construct all further strains.

Plasmid construction and transformation. The plasmids used in this work are listed in Table 4. The *S. cerevisiae MDH3* gene was amplified by PCR from

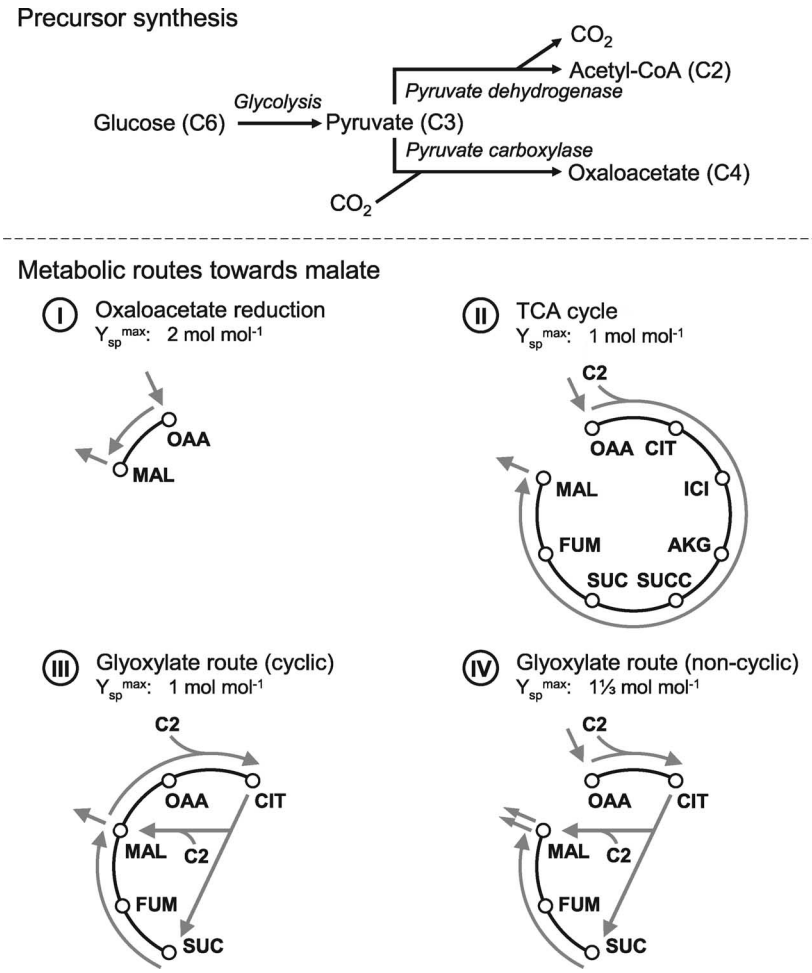

FIG. 1. Four possible pathways for malate production in *S. cerevisiae*, using oxaloacetate and/or acetyl-CoA as precursors. (I) Direct reduction of oxaloacetate. (II) Oxidation of citrate via the TCA cycle. (III) Formation from acetyl-CoA via the cyclic glyoxylate route. (IV) Formation from acetyl-CoA and oxaloacetate via the noncyclic glyoxylate route. OAA, oxaloacetate; MAL, malate; CIT, citrate; ICI, isocitrate; AKG, α-ketoglutarate; SUCC, succinyl-CoA; SUC, succinate; FUM, fumarate; C2, acetyl-CoA; Y_{sp}^{max}, maximum theoretical yield (in mol malate per mol glucose).

chromosomal DNA of *S. cerevisiae* CEN.PK113-7D using the primers XbaI-5′MDH3 and 3′MDH3-SalI. The resulting fragment contains the whole *MDH3* gene, except for the last 9 base pairs that encode the peroxisomal targeting sequence (the tripeptide SKL) (32). The PCR fragment was cut at the introduced XbaI and SalI sites and ligated to p426GPD that was digested with SpeI and XhoI, resulting in p426GPDMDH3ΔSKL. The cassette containing *MDH3ΔSKL* flanked by the *TDH3* promoter and the *CYC1* terminator was cut from p426GPDMDH3ΔSKL using KpnI and SacI. The ends were made blunt using mung bean nuclease (New England BioLabs, Beverly, MA) according to the manufacturer's protocol, followed by ligation of the fragment into the multicopy plasmid pRS2 (which carries *S. cerevisiae PYC2*) (47) cut with SmaI. This resulted in pRS2MDH3ΔSKL.

The gene coding for the *Schizosaccharomyces pombe* malate transporter, Sp*MAE1*, was amplified by PCR from chromosomal DNA of *S. pombe* L972 using primers XbaI-5′SpMAE1 and 3′SpMAE1-SalI. The resulting fragment was digested with XbaI and SalI and ligated into p425GPD cut with SpeI and XhoI. This resulted in p425GDPSpMAE1, which was then digested with KpnI and SacI to obtain the cassette with the *TDH3* promoter, Sp*MAEI*, and the *CYC1* terminator. The cassette was ligated into the multicopy plasmid YEplac112 that was also digested with KpnI and SacI, resulting in YEplac112SpMAE1.

Restriction endonucleases (New England BioLabs and Roche, Basel, Switzerland) and DNA ligase (Roche) were used according to instructions supplied by the manufacturers. Plasmids were isolated from *Escherichia coli* with a QIAprep Spin miniprep kit (Qiagen, Hilden, Germany). DNA fragments were separated on a 1% agarose gel (Sigma, St. Louis, MO) in 1× Tris-borate-EDTA (44). Fragments were isolated from the gel using a QIAquick gel extraction kit (Qiagen). *MDH3ΔSKL* and Sp*MAE1* were amplified using $Vent_R$ DNA polymerase (New England BioLabs) according to the manufacturer's instructions. PCR was performed with a Biometra TGradient thermocycler (Biometra, Göttingen, Germany) in 30 consecutive cycles of annealing (1 min at 60°C), extension (3 min at 75°C), and denaturation (1 min at 94°C).

Plasmids were amplified in *E. coli* XL1 Blue (Stratagene, La Jolla, CA). *E. coli* transformations were performed according to the method described by Inoue et al. (25). For plasmid isolations, *E. coli* was grown on Luria-Bertani plates or in liquid Terrific broth medium (44). Yeast transformations were performed according to the method described by Gietz and Woods (18). After transformation of RWB961 with the various plasmids, the yeast strains were plated on solid MYD.

Shake flask cultivation. Shake flask cultures were grown on synthetic medium, consisting of demineralized water and 100 g liter^{-1} glucose, 3 g liter^{-1} KH_2PO_4, 6.6 g liter^{-1} K_2SO_4, 0.5 g liter^{-1} $MgSO_4 \cdot 7\ H_2O$, and 1 ml trace element solution (56). For the ^{13}C-NMR analyses, 100 g liter^{-1} D-[1-^{13}C]glucose (99% ^{13}C labeling purity; Campro Scientific GmbH, Germany) was used. After the pH was set to 4.8 with KOH and the solution was heat sterilized for 20 min at 110°C, a filter-sterilized vitamin solution (56) (1 ml liter^{-1}) and urea (to a final concentration of 1 g liter^{-1}) were added. Urea was used as the only nitrogen source in all experiments to avoid additional acidification of the medium by ammonium uptake, which especially for precultures was undesired. Shortly before inoculation with 1 g liter^{-1} of biomass dry weight, medium (100 ml) was added to sterile 500-ml round-bottom flasks containing 5 g of $CaCO_3$, as dissolving of $CaCO_3$ would otherwise lead to a too-high initial pH. Shake flasks were incubated at 30°C and 200 rpm in a rotary shaker. For shake flask cultivations starting with

TABLE 2. *S. cerevisiae* strains used in this study[a]

Strain	Genotype
CEN.PK 113-7D	*MAT***a**, wild-type reference strain
TAM *ura3*Δ	*MAT***a** *pdc1*(*-6,-2*)::*loxP pdc5*(*-6,-2*)::*loxP pdc6*(*-6,-2*)::*loxP mutx ura3-52*; selected for C_2 independence in glucose-limited chemostats and glucose-tolerant growth in batch culture
RWB961 *ura3*Δ *trp1*Δ	*MAT***a** *pdc1*(*-6,-2*)::*loxP pdc5*(*-6,-2*)::*loxP pdc6*(*-6,-2*)::*loxP mutx ura3-52 trp1*::*Kanlox*
RWB961 empty vector	*MAT***a** *pdc1*(*-6,-2*)::*loxP pdc5*(*-6,-2*)::*loxP pdc6*(*-6,-2*)::*loxP mutx ura3-52 trp1*::*Kanlox* {YEplac195, YEplac112}
RWB961 ↑*PYC2*	*MAT***a** *pdc1*(*-6,-2*)::*loxP pdc5*(*-6,-2*)::*loxP pdc6*(*-6,-2*)::*loxP mutx ura3-52 trp1*::*Kanlox* {pRS2, YEplac112}
RWB961 ↑*MDH3*Δ*SKL*	*MAT***a** *pdc1*(*-6,-2*)::*loxP pdc5*(*-6,-2*)::*loxP pdc6*(*-6,-2*)::*loxP mutx ura3-52 trp1*::*Kanlox* {p426GPDMDH3ΔSKL, YEplac112}
RWB961 ↑Sp*MAE1*	*MAT***a** *pdc1*(*-6,-2*)::*loxP pdc5*(*-6,-2*)::*loxP pdc6*(*-6,-2*)::*loxP mutx ura3-52 trp1*::*Kanlox* {p426GPD, YEplac112SpMAE1}
RWB961 ↑*PYC2* + ↑*MDH3*Δ*SKL*	*MAT***a** *pdc1*(*-6,-2*)::*loxP pdc5*(*-6,-2*)::*loxP pdc6*(*-6,-2*)::*loxP mutx ura3-52 trp1*::*Kanlox* {pRS2MDH3ΔSKL, YEplac112}
RWB961 ↑*MDH3*Δ*SKL* + ↑Sp*MAE1*	*MAT***a** *pdc1*(*-6,-2*)::*loxP pdc5*(*-6,-2*)::*loxP pdc6*(*-6,-2*)::*loxP mutx ura3-52 trp1*::*Kanlox* {p426GPDMDH3ΔSKL, YEplac112SpMAE1}
RWB961 ↑*PYC2* + ↑*SpMAE1*	*MAT***a** *pdc1*(*-6,-2*)::*loxP pdc5*(*-6,-2*)::*loxP pdc6*(*-6,-2*)::*loxP mutx ura3-52 trp1*::*Kanlox* {pRS2, YEplac112SpMAE1}
RWB525 ↑*PYC2* + ↑*MDH3*Δ*SKL* + ↑Sp*MAE1*	*MAT***a** *pdc1*(*-6,-2*)::*loxP pdc5*(*-6,-2*)::*loxP pdc6*(*-6,-2*)::*loxP mutx ura3-52 trp1*::*Kanlox* {pRS2MDH3ΔSKL, YEplac112SpMAE1}

[a] All strains except CEN.PK 113-7D are derived from the evolved Pdc$^-$ *S. cerevisiae* (TAM) strain.

200 g liter^{-1} glucose, 15 g of $CaCO_3$ was added per flask to prevent $CaCO_3$ depletion.

Precultures were grown under identical conditions except for the amounts of glucose (20 g liter^{-1}) and urea (2.3 g liter^{-1}), the pH (set to 6.0 with KOH), and the lack of $CaCO_3$. Preculture shake flasks were inoculated with 2 ml of stock culture. After 48 h of cultivation, the broth was centrifuged. The pellet was resuspended in 10 ml demineralized water, and the cell suspension was equally divided over two shake flasks with fresh preculture medium, in order to obtain more biomass. After an additional 24 h of cultivation, the biomass concentration was determined and the broth was centrifuged. Cells were resuspended in demineralized water, and shake flasks with production medium were inoculated with 2 ml of cell suspension to obtain an initial biomass dry weight of 1 g liter^{-1}.

Chemostat cultivation for in vitro enzyme activity assays. Aerobic nitrogen-limited chemostat cultivation was performed as described previously (52), at a dilution rate of 0.10 h^{-1} and with 32 g liter^{-1} glucose in the chemostat medium. For each chemostat, a shake flask with 100 ml preculture medium (see above for medium composition) was inoculated with 2 ml of stock culture. After 48 h of cultivation, the broth was transferred wholly to a fermentor containing 1 liter of medium. The fermentor was switched to the chemostat regimen after completion of the batch phase. When steady-state conditions were obtained, cultures were sampled for in vitro enzyme activity measurements.

Dry weight determination. Culture samples (5 ml) were filtrated over oven-dried and weighed nitrocellulose filters (0.45-μm pore size; Pall Corporation) and washed with demineralized water. Biomass dry weight concentrations were determined from the weight increase after filters were dried in a microwave oven for 20 min at 360 W. Before dry weight determination, excess $CaCO_3$ was dissolved by acidification of the broth with 0.2 M HCl.

TABLE 3. Oligonucleotides used in this study

Oligonucleotide	Sequence
KanA	CGCACGTCAAGACTGTCAAG
KanB	TCGTATGTGAATGCTGGTCG
5′trp1::kanlox	GCCAAGAGGGAGGGCATTGGTGACTA TTGAGCACGTGAGTATAC
3′trp1::kanlox	GAACTATTTTTATATGCTTTTACAAGAC TTGAAATTTTCCTTGC
5′TRP1	TGGCATGTCTGGCGATGATA
3′TRP1	CGCCTGTGAACATTCTCTTC
XbaI-5′MDH3	GCTCTAGAAACATGGTCAAAGTCGCAA
3′MDH3-SalI	AGCTGTCGACTCAAGAGTCTAGGATGA AACTCT
XbaI-5′SpMAE1	GCTCTAGACATGGGTGAACTCAAGGA
3′SpMAE1-SalI	ACGCGTCGACTTAAACGCTTTCATG TTCA

Metabolite analysis. Extracellular concentrations of acetate, ethanol, fumarate, glucose, glycerol, lactate, and succinate were determined by high-performance liquid chromatography (HPLC), using a Bio-Rad Aminex HPX-87H column eluted with 5 mM H_2SO_4, at a flow rate of 0.6 ml min^{-1} and at 60°C. Acetate, fumarate, and lactate were detected by a Waters 2487 dual-wavelength absorbance detector at 214 nm. Ethanol, glucose, glycerol, and succinate were detected with a Waters 2410 refractive index detector. Malate was determined by enzymatic analysis (Enzyplus L-malic acid kit no. EZA786; Raisio Diagnostics). Pyruvate was assayed enzymatically with a reaction mixture containing 100 mM potassium phosphate buffer (pH 7.5), 0.17 mM NADH, and diluted culture supernatant. Pyruvate was determined by measuring NADH consumption after the addition of lactate dehydrogenase (6 U ml^{-1}).

Preparation of cell extracts for in vitro enzyme activity assays. Steady-state chemostat samples were centrifuged, washed, and resuspended in potassium phosphate buffer (10 mM, pH 7.5, with 2 mM EDTA) and stored at −20°C. Before being assayed, samples were thawed, washed, and resuspended in potassium phosphate buffer (100 mM, pH 7.5; with 2 mM $MgCl_2$ and 1 mM dithiothreitol). Extracts were prepared with a FastPrep 120A (Thermo Scientific) using 0.75 g glass beads (G8772; Sigma) per ml of cell suspension in four bursts (20 s per burst at speed 6, with 60-s intervals to allow for cooling). Unbroken cells and debris were removed by centrifugation (4°C, 20 min, 47,000 × *g*). The supernatant was used for the enzyme activity assays.

In vitro enzyme activity assays. The assay mixture for malate dehydrogenase contained 0.1 M potassium phosphate buffer (pH 8.0) and 0.15 mM NADH in demineralized water. The reaction was started by the addition of 1 mM oxaloacetate. Malate dehydrogenase activity was measured spectrophotometrically by monitoring NADH oxidation at 340 nm. Activities of pyruvate carboxylase, isocitrate lyase, and phosphoenolpyruvate carboxykinase were determined as described previously (10). All enzymes activities were measured at 30°C. Protein concentrations in cell extracts were determined by the Lowry method (29) using bovine serum albumin as the standard.

NMR measurements. D_2O (0.1 ml, 99.9%; Isotec) was added to a 0.4-ml sample in a 5-mm NMR tube. One-dimensional ^{1}H- and ^{13}C-NMR spectra were obtained at, respectively, 500 and 125 MHz with a probe temperature of 280 K on a Bruker AMX-500 spectrometer, located at the Wageningen NMR Centre. ^{13}C enrichments were calculated from the ^{1}H spectrum by comparing the signal of the ^{13}C satellites to the total signal obtained for the proton attached to the carbon of interest. ^{13}C enrichments of carbon atoms that were part of carboxyl groups, which lack an adjacent proton, were calculated from the ^{13}C-NMR

TABLE 4. Plasmids used in this study

Plasmid	Characteristics	Reference
p425GPD	2μm *LEU2*, P_{TDH3}	Mumberg et al. (36)
p426GPD	2μm *URA3*, P_{TDH3}	Mumberg et al. (36)
p426GPDMDH3ΔSKL	2μm *URA3*, P_{TDH3}-*MDH3ΔSKL*	This work
p425GPDSpMAE1	2μm, *LEU2*, P_{TDH3}-*S. pombe MAE1*	This work
pRS2	2μm, *URA3 PYC2*	Stucka et al. (47)
pRS2MDH3ΔSKL	2μm, *URA3 PYC2*, P_{TDH3}-*MDH3ΔSKL*	This work
pUG6	*loxP*-KanMX-*loxP* cassette	Güldener et al. (22)
YEplac195	2μm, *URA3*	Gietz and Sugino (17)
YEplac112	2μm, *TRP1*	Gietz and Sugino (17)
YEplac112SpMAE1	2μm, *TRP1*, P_{TDH3}-*S. pombe MAE1*	This work

spectra by comparing the signal of these carbon atoms in a completely relaxed spectrum to the signal obtained for other carbon atoms within the same compound for which ^{13}C enrichments could be determined using ^{1}H spectra. The ^{13}C-enrichment data for succinate were not included in the analysis, as these enrichments could not be determined accurately due to overlapping signals in the NMR spectra of succinate and other compounds.

^{13}C-labeling-based metabolic flux analysis. By iteratively fitting fluxes in a metabolic model, a set of fluxes could be estimated that yielded ^{13}C-enrichment data similar to the measured NMR data, while satisfying the mass balances of the model. The mass balances followed from the model stoichiometry and incorporated the measured consumption and production rates of carbon-containing compounds. These included the consumption rate of glucose and the production rates of malate, succinate, fumarate, pyruvate, glycerol, and biomass.

The metabolic model used (see Table SA1 in the supplemental material) (see Fig. 4) was based on the *S. cerevisiae* genome-scale metabolic model of Duarte et al. (11). Compartmentalization was limited to the cytosol and mitochondrion. Cytosolic reactions include glycolysis and the pentose-phosphate pathway (modeled according to Kleijn et al.) (27) as well as relevant cytosolic reactions involving C_4-dicarboxylic acids. The mitochondrial compartment contains the reactions of the TCA cycle. Since the model contains only one (cytosolic) carbon dioxide-consuming reaction, a single spatially homogeneous carbon dioxide pool was used in the model which, in addition to influxes of the modeled carbon dioxide-producing metabolic reactions, included an additional influx of nonenriched carbon dioxide to account for the dissolution of the calcium carbonate. The stoichiometry of carbon dioxide export, the result of respiratory glucose dissimilation, was calculated from the carbon balance. The gluconeogenic phosphoenolpyruvate carboxykinase reaction was not included in the model, as this enzyme is subject to glucose repression and inactivation (15), and its presence could lead to cycling between pyruvate and phosphoenolpyruvate. Scrambling reactions were included to distribute labeling of the symmetric compounds succinate and fumarate evenly over their symmetric carbon atoms. Where possible, the model was simplified by combining reactions. Reversible reactions were modeled as separate forward and backward reactions. Exchange fluxes between the cytosol and mitochondria were unrestricted in all calculations.

Consumption rates of macromolecule precursors were included in the model to account for the demand of these precursors in biomass formation. The consumption rates of these precursors were estimated using the macromolecular biomass composition (28) at the estimated specific growth rate, combined with the stoichiometric precursor requirements for macromolecule construction as listed in the metabolic model of Daran-Lapujade et al. (8).

A previously described flux fitting procedure (55) was used. The sum of squared residuals (SS_{res}) between the simulated and measured data was minimized using sequential quadratic programming, implemented in Matlab (R2006b; The MathWorks, Inc.). End-point labeling patterns of extracellular metabolites were used to gain insight into the overall, time-averaged contribution of specific pathways to malate production. This approach does not allow for the analysis of possible changes in flux distribution during the experiment.

RESULTS

Overproduction of pyruvate carboxylase, cytosolically relocated malate dehydrogenase, and *S. pombe* malate permease. The metabolic engineering strategy that was explored in this study is based on the high-level expression of three proteins. To overexpress pyruvate carboxylase, the multicopy plasmid pRS2, which carries the *PYC2* gene under the control of its native promoter (47), was used. In *S. cerevisiae*, pyruvate carboxylase is a cytosolic enzyme (23, 43, 54, 60). Therefore, to circumvent the need for transport of oxaloacetate and malate between subcellular compartments, malate dehydrogenase should preferably also be expressed in the cytosol. One of the three malate dehydrogenase isoenzymes in *S. cerevisiae*, Mdh2p, is located in the cytosol. However, Mdh2p is subject to glucose catabolite inactivation (33, 35), which is an undesirable property for batch cultivation on glucose. Therefore, the strategy for cytosolic malate dehydrogenase overexpression was based on retargeting the peroxisomal isoenzyme encoded by *MDH3*. Peroxisomal targeting of Mdh3p is caused by a C-terminal SKL tripeptide (32). An *MDH3* allele, in which the 9 nucleotides that encode this C-terminal sequence were removed, was cloned in multicopy vectors under the control of the constitutive *TDH3* promoter (Table 4). Subcellular fractionation experiments on aerobic, glucose-limited chemostat cultures, performed as described by Luttik et al. (31), confirmed that overexpression of the truncated *MDH3* resulted in a >20-fold increase in cytosolic malate dehydrogenase activity (data not shown).

It has previously been reported that transport of malate across the plasma membrane of *S. cerevisiae* occurs at very low rates, probably via diffusion (58). As insufficient transport capacity might impede efficient production of malate, the *S. pombe* malate transporter SpMae1p (21), which has been demonstrated to mediate both import and export of malate when expressed in *S. cerevisiae* (5, 59), was expressed under the control of the *TDH3* promoter from a separate multicopy plasmid.

The expression cassettes were introduced in an evolved pyruvate-overproducing Pdc^- *S. cerevisiae* strain (53), resulting in strain RWB525 (Table 2). To confirm overexpression of Pyc2 and Mdh3ΔSKL in this strain that also carried the Sp*MAE1* expression vector, pyruvate carboxylase and malate dehydrogenase activities were analyzed using cell extracts of aerobic, nitrogen-limited chemostat cultures grown at a dilution rate of 0.10 h^{-1}. Pyruvate carboxylase and malate dehydrogenase activities were 0.24 ± 0.02 and 30.5 ± 0.6 μmol min^{-1} (mg protein)$^{-1}$, respectively. These activities were about 10-fold higher than those of an empty vector (YEplac195) reference strain, for which pyruvate carboxylase and malate dehydrogenase activities were 0.02 ± 0.00 and 3.5 ± 0.1 μmol min^{-1} (mg protein)$^{-1}$, respectively.

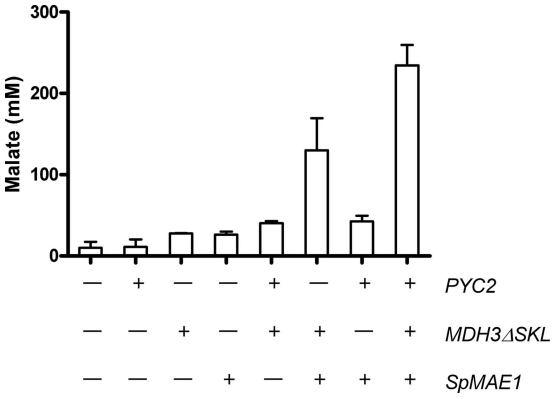

FIG. 2. Malate concentrations obtained in shake flask cultivations of different strains of *S. cerevisiae* overexpressing combinations of pyruvate carboxylase, malate dehydrogenase, or malate permease. Concentrations were determined after 96 h of cultivation when glucose was depleted (100 ml synthetic medium in 500-ml shake flasks, 100 g liter^{-1} glucose, 5 g $CaCO_3$). Each bar represents a strain. A plus sign (+) below the bar indicates that the gene shown at the end of the row (*PYC2*, *MDH3*Δ*SKL*, or Sp*MAE1*) is overexpressed in that particular strain. If a minus sign (−) is listed, the gene was not overexpressed. Error bars indicate standard deviations (each strain was tested at least twice).

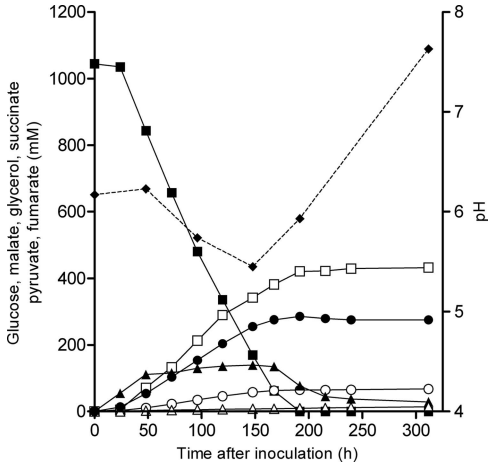

FIG. 3. Extracellular metabolite concentrations during a representative shake flask fermentation of RWB525 (100 ml synthetic medium in a 500-ml shake flask, 188 g liter^{-1} initial glucose, 15 g $CaCO_3$, 1 g liter^{-1} initial biomass). Glucose (■), malate (□), glycerol (●), succinate (○), pyruvate (▲), fumarate (△), and pH (◆; dashed line) are shown. End point determinations of two additional experiments yielded quantitatively similar results. Standard deviations for these experiments are indicated in the text.

Impact of pyruvate carboxylase, malate dehydrogenase, and malate permease on malate production. To study the individual and combined effects of the different genetic modifications on malate production, a set of prototrophic strains (Table 2) with different combinations of *PYC2*-, *MDH3*Δ*SKL*- and Sp*MAE1*-carrying plasmids was tested in shake flasks on synthetic medium containing 100 g liter^{-1} glucose (Fig. 2). To prevent acidification, calcium carbonate was added as a buffering agent. The addition of 50 g liter^{-1} of $CaCO_3$ ensured saturation throughout the fermentation. Shake flasks were sampled 4 days after inoculation, when glucose depletion was confirmed by HPLC. Under these conditions, the pyruvate decarboxylase-negative host strain *S. cerevisiae* TAM produced ca. 10 mM malate. Control experiments showed that after glucose depletion, malate consumption was negligible.

Overexpression of *PYC2* alone had only a small impact on malate production (Fig. 2). Conversely, individual overexpression of either *MDH3*Δ*SKL* or Sp*MAE1* led to a ca. threefold increase of the malate concentration reached in the shake flask fermentation experiments. This result indicates that pyruvate carboxylase has a low degree of control over the rate of malate production in the reference strain.

Even in combination with either *MDH3*Δ*SKL* or Sp*MAE1*, overexpression of *PYC2* yielded only small increases of the malate titer relative to strains in which *MDH3*Δ*SKL* or Sp*MAE1* were expressed individually (Fig. 2). In contrast, the combined overexpression of *MDH3*Δ*SKL* and Sp*MAE1* resulted in a >10-fold increase of the malate titer relative to that for the Pdc$^-$ reference strain (130 ± 39 mM). The highest malate concentrations (235 ± 25 mM) were obtained with strain RWB525, in which *PYC2*, *MDH3*Δ*SKL*, and Sp*MAE1* were simultaneously overexpressed. These results suggest that as malate dehydrogenase and a malate exporter are overexpressed, the control of malate production shifts to pyruvate carboxylase. HPLC analysis of culture supernatants showed that in addition to malate, the engineered strains produced substantial amounts of glycerol, pyruvate, and succinate.

Product formation by strain RWB525 in shake flask cultures. In the experiments shown in Fig. 2, the emphasis was on final malate titers. The kinetics of malate production and byproduct formation were investigated in more detail for strain RWB525, in which *PYC2*, *MDH3*Δ*SKL*, and Sp*MAE1* were simultaneously overexpressed. In $CaCO_3$-buffered shake flask cultures grown on 189 ± 1 g liter^{-1} glucose, a final concentration of 59 ± 2 g liter^{-1} malic acid was obtained, corresponding to an overall malate yield on glucose of 0.42 mol mol^{-1} (Fig. 3). For the fermentation shown in this figure, the average volumetric malate production rate was 0.29 g liter^{-1} h^{-1} during the period of glucose consumption, the first 192 h of incubation.

In addition to malate, the engineered strain produced succinic acid (8 ± 0 g liter^{-1}), glycerol (25 ± 0 g liter^{-1}), pyruvic acid (3 ± 0 g liter^{-1}), and fumaric acid (2 ± 0 g liter^{-1}). The concentrations of succinate, glycerol, and fumarate increased at rather constant rates during glucose consumption and remained constant following glucose depletion. Pyruvate was produced mainly in the first 50 h of the fermentation. After reaching a concentration of 12 g liter^{-1} (Fig. 3), pyruvate was partially consumed again after glucose was depleted.

The culture pH, which remained between 5.5 and 6.5 during the glucose consumption phase, increased after glucose depletion (Fig. 3). The observed pH profile can be explained by taking into account the presence of $CaCO_3$ and the production or consumption of acids. When a saturating amount of $CaCO_3$ is added to the synthetic medium, which has a low buffering capacity, dissolving $CaCO_3$ will increase the pH to a value of around 8 at equilibrium. The small initial increase in pH during the lag phase of fermentation (Fig. 3) can therefore be explained by the dissolving $CaCO_3$. During the glucose consump-

tion phase, the production of acids results in a net decrease in pH. Finally, after glucose depletion, the pH increased again due to consumption of pyruvate and dissolving $CaCO_3$ (Fig. 3).

Verification of the malate production pathway. The malate yield of 0.42 mol (mol glucose)$^{-1}$ reached in the batch experiments with strain RWB525 did not surpass the maximum theoretical yields of the less-efficient pathways. For the design of future optimization studies, it is important to know whether the less-efficient, oxidative pathways contribute to malate production by the engineered strains.

To test whether the glyoxylate routes contributed to malate formation by strain RWB525, the activity of the crucial enzyme isocitrate lyase was measured using cell extracts of malate-producing shake flask cultures. Isocitrate lyase activity was below the detection limit of the assay (0.005 μmol min^{-1} [mg protein]$^{-1}$), whereas positive controls (RWB525 and the wild-type reference strain grown on ethanol) reproducibly showed isocitrate lyase activities of 0.1 to 0.2 μmol min^{-1} (mg protein)$^{-1}$ which, for the reference strain, are in good agreement with literature values (9). The absence of detectable isocitrate lyase activity is consistent with the fact that this enzyme is subject to glucose catabolite inactivation (37) and was taken as evidence that the glyoxylate routes do not contribute to malate production by strain RWB525. Similarly, phosphoenolpyruvate carboxykinase activities in these cell extracts were below the detection limit of the assay (0.005 μmol min^{-1} [mg protein]$^{-1}$), whereas a positive control of the wild-type reference strain grown on ethanol showed an activity of 0.4 μmol min^{-1} (mg protein)$^{-1}$.

Enzyme activities cannot be used to assess the contribution of the nonoxidative pathway and oxidative formation of malate via the TCA cycle. Therefore, a ^{13}C-NMR-based metabolic flux analysis was performed with strain RWB525 grown in shake flask cultures on 100 g liter^{-1} [1-^{13}C]glucose. This approach, based on the dependency of ^{13}C labeling patterns of extracellular metabolites on the intracellular fluxes, has been applied previously to study pathways of malate formation in strains of *A. flavus* and *S. cerevisiae* (38, 40).

After 3 days, when no residual [1-^{13}C]glucose could be detected, culture supernatants were analyzed by NMR. Enrichments were measured for malate, succinate, fumarate, glycerol, and pyruvate. Two types of ^{13}C-enrichment data were obtained: positional, indicating ^{13}C enrichment at specific carbon positions (e.g., the C-2 of malate), and relative, indicating the fraction of molecules, ^{13}C labeled at carbon position A, that are also ^{13}C labeled at neighboring position B (Table 5). Flux analyses were performed using both physiological and enrichment data combined with a metabolic model, as described by Wiechert (62). The metabolic model consisted of glycolysis, the pentose phosphate pathway (PPP), the TCA cycle, and the relevant reactions of cytosolic C_4-dicarboxylic acid metabolism. Based on the absence of measurable isocitrate lyase and phosphoenolpyruvate carboxykinase activities (see above), the glyoxylate cycle and the phosphoenolpyruvate carboxykinase reaction were omitted from the model.

The measured consumption and production rates for glucose, malate, succinate, fumarate, pyruvate, and glycerol were used as constraints for the mass balances of the metabolic model. The increase in biomass concentration was 6 g of dry weight liter^{-1}, as determined by using two shake flasks with non-^{13}C-enriched glucose. An estimated average specific growth rate in the cultures of 0.10 h^{-1} was used to estimate the consumption rates of precursors for biomass formation.

TABLE 5. ^{13}C enrichments of metabolites in the supernatant[a]

Metabolite	^{13}C enrichment		Enrichment percentage		
	Type	Location[b]	Measured		Fitted
			Expt I	Expt II	
Pyruvate	Positional	C-2	1	1	1
		C-3 (δ 1.43)	46	46	45
		C-3 (δ 1.34)	46	45	45
Malate	Positional	C-1	5	ND	5
		C-2	15	15	17
		C-3	33	32	32
		C-4	6	ND	5
	Relative	C-1 given that C-2	5	4.5	6
		C-2 given that C-1	21	20	19
		C-2 given that C-3	4	4	5
		C-3 given that C-2	10	10	10
		C-3 given that C-4	28	30	31
		C-4 given that C-3	5	4.5	4
Glycerol	Positional	C-1/C-3 (δ 3.48)	26	25	25
		C-1/C-3 (δ 3.57)	25	23	25
		C-2	1	1	1
Fumarate	Positional	C-2/C-3	25	25	25

[a] The supernatant was sampled after 72 h of cultivation in shake flasks containing pure [1-^{13}C]glucose. The estimated error for the determination of the ^{13}C enrichments is 1% (absolute to the measurement). Positional ^{13}C enrichments indicate the enrichment at specific carbon positions. Relative enrichments indicate the fraction of molecules, ^{13}C labeled at carbon position A, that are also ^{13}C labeled at neighboring position B. This is presented as "B given that A." ND, not determined.

[b] Chemical shifts (δ, in ppm) are given in parentheses.

The obtained optimal fit for flux distribution in strain RWB525 represents a situation in which all excreted malate is derived via the nonoxidative pathway, i.e., by carboxylation of pyruvate and the subsequent reduction of oxaloacetate to malate by malate dehydrogenase (Fig. 4). In this situation, the TCA cycle supplies only the excreted succinate, and mitochondrial pyruvate is supplied by mitochondrial import of cytosolic pyruvate and by malic enzyme. The mitochondrial malate required for the latter reaction is supplied by mitochondrial import of cytosolic fumarate followed by its conversion to mitochondrial malate. The minimized covariance-weighted sum of squared residuals (the flux-fit error) between the measured and fitted ^{13}C enrichments was 8. Deviations of 1% (absolute) between all measured and simulated enrichment percentages (which is the estimated measurement error) would have resulted in an error of 15.

The estimated flux distribution shown in Fig. 4 was consistent with exclusive involvement of the envisaged nonoxidative pathway. However, it remained relevant to assess to what extent an involvement of the oxidative TCA cycle pathway would result in a worse fit of the ^{13}C-enrichment data. To this end, a sensitivity analysis was performed by fixing the net cytosolic malate dehydrogenase and malic enzyme fluxes in the model to reduced values, while allowing the optimization algorithm to change the remaining fluxes to minimize the fitting error. The malic enzyme flux was included in this sensitivity analysis, since

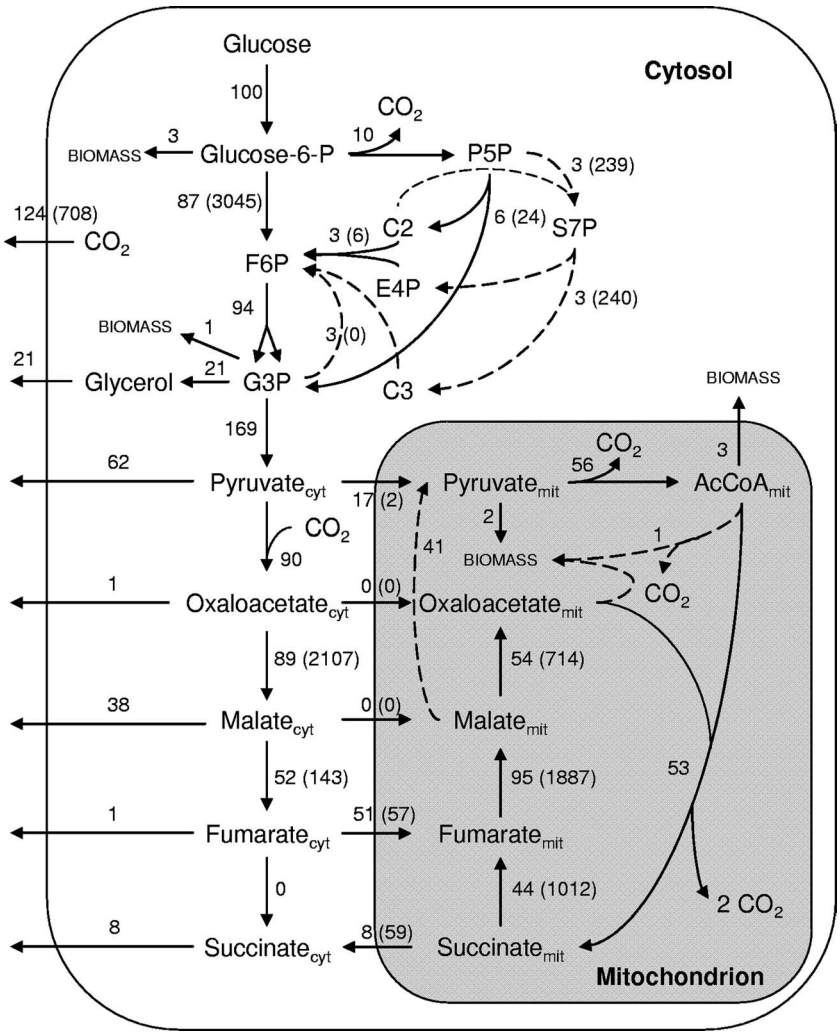

FIG. 4. Flux estimates for the ^{13}C-based metabolic flux analysis of RWB525 under malate-producing conditions in shake flasks. Fluxes (in moles) are normalized for a glucose uptake of 100 mol. Arrows indicate the direction of the (net) flux. In the case of reversible reactions, the exchange flux is included in parentheses. Some arrows are dashed to improve readability. Metabolites present in both compartments are differentiated by the indicators "cyt" (cytosol) and "mit" (mitochondrion).

this flux has a large influence on the amount of freedom in the model, and in vitro enzyme activity measurements for malic enzyme were unsuccessful, probably due to interference by $CaCO_3$ (data not shown). The flux-fit error increased at low malic enzyme and low net cytosolic malate dehydrogenase fluxes (Fig. 5). For the extreme case where both these fluxes were set to zero, all excreted C_4-dicarboxylic acids were derived from the TCA cycle (Fig. 6, upper values in each set of three values). The flux-fit error for this condition increased from 8 for the best fit to 160, over 10 times higher than expected based on measurement error alone. When the malic enzyme flux was set to zero but the malate dehydrogenase flux was left free, the best fit represented a situation where the TCA cycle supplied the excreted succinate and fumarate, but the nonoxidative pathway still provided 94% of all excreted malate (Fig. 6, middle values). The flux-fit error for this situation was 18, double the flux-fit error for the best fit. In the other extreme scenario, the net cytosolic malate dehydrogenase flux was forced to zero, while the malic enzyme flux was fixed at the value obtained for the fit shown in Fig. 4. In this scenario, 35% of the excreted malate was produced via the nonoxidative pathway, while the remainder was produced via the oxidative TCA pathway (Fig. 6, lower values). In this case, all succinate and fumarate were derived from the TCA cycle. For this situation, the flux-fit error was 12, 1.5-fold higher than the flux-fit error for the best fit.

DISCUSSION

Contribution of different pathways to malate production. High-yield production of malate by engineered *S. cerevisiae* strains requires the exclusive use of the nonoxidative pathway of malate production. While involvement of the glyoxylate pathways could be excluded based on enzyme activity assays, this method was not applicable for analyzing involvement of the oxidative TCA cycle pathway. Use of [1-^{13}C]glucose to distinguish between the production of malate via the nonoxidative route and oxidative TCA cycle pathways has been de-

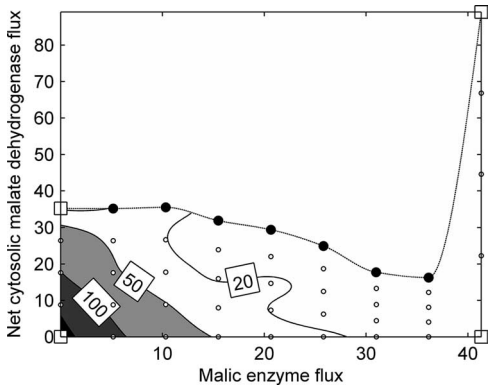

FIG. 5. Sensitivity analysis showing the covariance-weighted sum of squared residuals (the flux-fit error) between measured and fitted ^{13}C-enrichment data over a range of malic enzyme and net cytosolic malate dehydrogenase fluxes. Optimizations were run at various fixed malic enzyme fluxes. For each malic enzyme flux, the net cytosolic malate dehydrogenase was forced stepwise from the free fit value to lower values. Flux distributions of the square data points are shown in detail in Fig 4 and 6: the top right point represents the best fit (Fig. 4), the lower left, top left, and lower right are, respectively, the upper, middle, and lower values in Fig. 6. The black surface in the lower left of the figure contains errors higher than 150.

scribed previously (38). That approach was based on the assumptions that conversion of [1-^{13}C]glucose through the nonoxidative pathway yields [3-^{13}C]malate, that the oxidative glyoxylate pathway would yield [2,3-^{13}C]malate, and that the oxidative TCA cycle pathway would result in the formation of [1,2,3,4-^{13}C]malate. Strong ^{13}C enrichment of malate at the C-3 atom would then be indicative of an active nonoxidative pathway (38).

Several effects may complicate the above interpretation of ^{13}C-labeling patterns of malate. First, $^{13}CO_2$, a product of the oxidative PPP, can participate in carboxylation reactions. Second, the nonoxidative part of the PPP yields [1,2,3-^{13}C]pyruvate (27). Moreover, reversible reactions often result in more-complex labeling. For example, even in the absence of a net flux, malate dehydrogenase activity can equilibrate the labeling patterns of oxaloacetate and malate. Oxaloacetate can then be used in the oxidative TCA or glyoxylate cycle pathways. Alternatively, interconversion of malate and fumarate by fumarase may result in redistribution of malate labeling due to the symmetry of fumarate. These "scrambling" effects are especially relevant when, as is the case in the present study, malate yields are significantly lower than the maximum theoretical yield. These complications were taken into account in the metabolic flux analysis performed in this study. Their impact can, for instance, be seen in the optimal fit scenario (Fig. 4), in which all excreted malate is derived from the nonoxidative pathway, but the calculated ^{13}C labeling of the C-3 of malate was only 32%. This enrichment is much lower than the 51% enrichment that would be predicted when [1-^{13}C]glucose is converted solely via the nonoxidative pathway without interference of scrambling reactions. By taking into account the involvement of the PPP, which in the model results in a ^{13}C enrichment at the C-3 atom of pyruvate of only 45%, and a high fumarase exchange flux, resulting in redistribution of the ^{13}C label over the C-2 and C-3 carbon atoms of malate, it was nevertheless fully compatible with the exclusive involvement of the nonoxidative pathway.

Although the best fit for the observed ^{13}C labeling patterns indicated an exclusive involvement of the nonoxidative pathway (Fig. 4), the flux-fit errors of alternative scenarios that involved a contribution of the oxidative TCA cycle pathway were not high enough to reject them. An argument in favor of a predominant role of the nonoxidative pathway in malate production is the strong positive effect of *MDH3*Δ*SKL* overexpression on malate production (Fig. 2). As malate dehydrogenase overexpression specifically targets the nonoxidative pathway, its key role in malate production seems difficult to reconcile with flux fits in which the oxidative TCA cycle pathway made a significant contribution and cytosolic malate dehydrogenase activities were low or absent (Fig. 6).

Metabolic engineering of *S. cerevisiae* for malate production. In a previous study, we developed a pyruvate decarboxylase-negative strain of *S. cerevisiae* that lacks two important phenotypic characteristics of such strains: the requirement for a C_2 compound and an inability to grow at high glucose concentrations (53). The results presented in this study confirm that this strain is a suitable platform for metabolic engineering: high levels of malate were produced under conditions that would result in vigorous alcoholic fermentation in wild-type strains.

The present study shows that the *S. pombe* malate transporter SpMae1p, which has previously been applied to metabolically engineer *S. cerevisiae* for improved malate uptake (5, 59), can also be used to facilitate malate export. Malate export was shown to be a crucial process in metabolic engineering of *S. cerevisiae* for malate production (Fig. 2). However, the requirement for a heterologous malate transporter was not absolute. Even in the absence of Sp*MAE1*, strains that overexpressed *PYC2* and especially *MDH3*Δ*SKL* produced higher concentrations of malate than the pyruvate decarboxylase-negative host strain (Fig. 2). Under the experimental conditions, the intra- and extracellular pH values were above the pK_a values of malate (3.40 and 5.11), with only a small fraction of malate present in its uncharged, fully undissociated form. As it is unlikely that malate anions can diffuse freely across the plasma membrane at a significant rate, these results suggest the presence of a low-capacity native malate exporter. Indeed, a dicarboxylate transporter in *S. cerevisiae* was recently identified (2) and was shown to transport succinate with competitive inhibition by malate.

The impact of overexpressing *PYC2* was generally small, except when *MDH3*Δ*SKL* or Sp*MAE1* was also overexpressed. This result can probably be explained by very low cytosolic malate dehydrogenase and malate transport activity in the host strain. In wild-type *S. cerevisiae*, Mdh2p, the cytosolic isoenzyme of malate dehydrogenase (34), is subject to glucose-induced proteolysis (46) and glucose repression at the mRNA level (50). In contrast, pyruvate carboxylase is an essential anaplerotic enzyme that is expressed at significant levels in glucose-grown cultures of wild-type *S. cerevisiae* (23, 43, 54, 60).

The highest malate yield achieved in this study (0.42 mol per mol glucose) is still significantly lower than both the maximal theoretical yield that can be achieved via reduction of oxaloacetate (2 mol per mol) or the actual yields that have been achieved with *A. flavus* (up to 1.26 mol per mol glucose), which

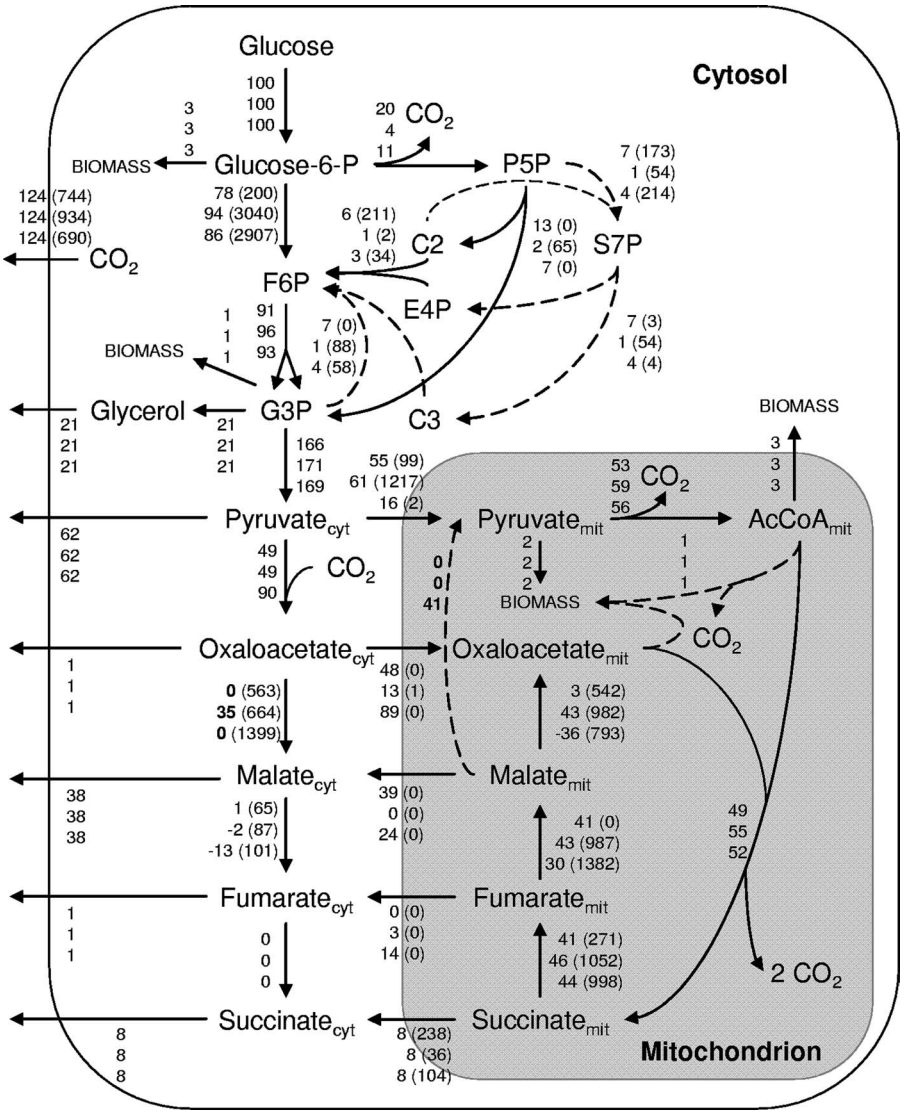

FIG. 6. Flux profiles for three highlighted situations from the sensitivity analysis of Fig. 5. Fluxes (in moles) are normalized for a glucose uptake of 100 mol. Arrows indicate the direction of the (net) flux. In case of reversible reactions, the exchange flux is included in parentheses. Some arrows are dashed to improve readability. Metabolites present in both compartments are differentiated by the indicators "cyt" (cytosol) and "mit" (mitochondrion). Upper numbers in each set of three, malic enzyme and net cytosolic malate dehydrogenase fluxes forced to 0; middle numbers, malic enzyme flux forced to 0; lower numbers, malic enzyme flux forced to the value obtained for the best fit and net cytosolic malate dehydrogenase flux forced to 0.

lacks "generally recognized as safe" (GRAS) status. Malate production in the best-performing *S. cerevisiae* strain (RWB525) was accompanied by respiratory dissimilation of glucose and the formation of pyruvate, glycerol, succinate, and fumarate. The residual production of pyruvate, the precursor for malate production and the main metabolite produced by the Pdc$^-$ host strain (53), indicates that the kinetics of the malate production pathway can still be further improved. Glycerol production is probably a consequence of the combination of a high rate of pyruvate production and a limited capacity for reoxidation of cytosolic NADH by mitochondrial respiration (3). This limitation may have been augmented by oxygen limitation, which readily occurs in shake flask cultures. With regard to succinate and fumarate, we observed higher concentrations of these acids after the introduction of SpMAE1p, suggesting that in addition to malate, SpMAE1p also mediates the export of succinate and fumarate. This observation is in agreement with earlier findings with *S. pombe*, where Sp*MAE1* is required for malic and succinic acid import (21). In addition, the overexpression of Sp*MAE1* in *S. cerevisiae* has been reported to enable import of malic, succinic, and fumaric acids (5).

The malate titers and yields achieved in this study are the highest that have hitherto been reported for *S. cerevisiae* (Table 1) and provide a good basis for further metabolic engineering of the production of C_4-dicarboxylic acids by *S. cerevisiae*. Analysis and improvement of the in vivo kinetics of malate production, as well as analysis of the pathways involved in

byproduct formation, will be important aspects of future research.

ACKNOWLEDGMENTS

The Ph.D. research of R.M.Z. is financed by Tate & Lyle Ingredients Americas. The Kluyver Centre for Genomics of Industrial Fermentation is supported by The Netherlands Genomics Initiative.

We thank Stanley Bower, Jefferson C. Lievense, Chi-Li Liu, Carlos Gancedo, Carmen-Lisette Flores, and Albert de Graaf for stimulating discussions. We acknowledge the contributions of Ann-Kristin Stave and Rosario F. Berriel to construction of the strains and of Marijke Luttik, Eline Huisjes, and Tiemen Zijlmans to subcellular localization experiments.

REFERENCES

1. **Abe, S., A. Furuya, T. Saito, and K. Takayama.** November 1962. Method of producing L-malic acid by fermentation. U.S. patent 3,063,910.
2. **Aliverdieva, D. A., D. V. Mamaev, D. I. Bondarenko, and K. F. Sholtz.** 2006. Properties of yeast *Saccharomyces cerevisiae* plasma membrane dicarboxylate transporter. Biochemistry (Moscow) **71:**1161–1169.
3. **Bakker, B. M., K. M. Overkamp, A. J. A. van Maris, P. Kotter, M. A. H. Luttik, J. P. van Dijken, and J. T. Pronk.** 2001. Stoichiometry and compartmentation of NADH metabolism in *Saccharomyces cerevisiae*. FEMS Microbiol. Rev. **25:**15–37.
4. **Battat, E., Y. Peleg, A. Bercovitz, J. S. Rokem, and I. Goldberg.** 1991. Optimization of L-malic acid production by *Aspergillus flavus* in a stirred fermentor. Biotechnol. Bioeng. **37:**1108–1116.
5. **Camarasa, C., F. Bidard, M. Bony, P. Barre, and S. Dequin.** 2001. Characterization of *Schizosaccharomyces pombe* malate permease by expression in *Saccharomyces cerevisiae*. Appl. Environ. Microbiol. **67:**4144–4151.
6. **Chibata, I., T. Tosa, and I. Takata.** 1983. Continuous production of L-malic acid by immobilized cells. Trends Biotechnol. **1:**9–11.
7. **Dakin, H. D.** 1924. The formation of *l*-malic acid as a product of alcoholic fermentation by yeast. J. Biol. Chem. **61:**139–145.
8. **Daran-Lapujade, P., M. L. A. Jansen, J. M. Daran, W. van Gulik, J. H. de Winde, and J. T. Pronk.** 2004. Role of transcriptional regulation in controlling fluxes in central carbon metabolism of *Saccharomyces cerevisiae*: a chemostat culture study. J. Biol. Chem. **279:**9125–9138.
9. **de Jong-Gubbels, P., J. Bauer, P. Niederberger, I. Stückrath, P. Kötter, J. P. van Dijken, and J. T. Pronk.** 1998. Physiological characterisation of a pyruvate-carboxylase-negative *Saccharomyces cerevisiae* mutant in batch and chemostat cultures. Antonie van Leeuwenhoek **74:**253–263.
10. **de Jong-Gubbels, P., P. Vanrolleghem, S. Heijnen, J. P. van Dijken, and J. T. Pronk.** 1995. Regulation of carbon metabolism in chemostat cultures of *Saccharomyces cerevisiae* grown on mixtures of glucose and ethanol. Yeast **11:**407–418.
11. **Duarte, N. C., M. J. Herrgard, and B. O. Palsson.** 2004. Reconstruction and validation of *Saccharomyces cerevisiae* iND750, a fully compartmentalized genome-scale metabolic model. Genome Res. **14:**1298–1309.
12. **Fatichenti, F., G. A. Farris, P. Deiana, and S. Ceccarelli.** 1984. Malic acid production and consumption by selected strains of *Saccharomyces cerevisiae* under anaerobic and aerobic conditions. Appl. Microbiol. Biotechnol. **19:** 427–429.
13. **Flikweert, M. T., M. de Swaaf, J. P. van Dijken, and J. T. Pronk.** 1999. Growth requirements of pyruvate-decarboxylase-negative *Saccharomyces cerevisiae*. FEMS Microbiol. Lett. **174**:73–79.
14. **Flikweert, M. T., L. Van der Zanden, W. M. T. M. Janssen, H. Y. Steensma, J. P. van Dijken, and J. T. Pronk.** 1996. Pyruvate decarboxylase: an indispensable enzyme for growth of *Saccharomyces cerevisiae* on glucose. Yeast **12:**247–257.
15. **Gancedo, C., and K. Schwerzmann.** 1976. Inactivation by glucose of phosphoenolpyruvate carboxykinase from *Saccharomyces cerevisiae*. Arch. Microbiol. **109:**221–225.
16. **Geiser, D. M., J. I. Pitt, and J. W. Taylor.** 1998. Cryptic speciation and recombination in the aflatoxin-producing fungus *Aspergillus flavus*. Proc. Natl. Acad. Sci. USA **95:**388–393.
17. **Gietz, R. D., and A. Sugino.** 1988. New yeast-*Escherichia coli* shuttle vectors constructed with *in vitro* mutagenized yeast genes lacking six-base pair restriction sites. Gene **74:**527–534.
18. **Gietz, R. D., and R. A. Woods.** 2002. Transformation of yeast by lithium acetate/single-stranded carrier DNA/polyethylene glycol method. Methods Enzymol. **350:**87–96.
19. **Giorno, L., E. Drioli, G. Carvoli, A. Cassano, and L. Donato.** 2001. Study of an enzyme membrane reactor with immobilized fumarase for production of L-malic acid. Biotechnol. Bioeng. **72:**77–84.
20. **Goldberg, I., J. S. Rokem, and O. Pines.** 2006. Organic acids: old metabolites, new themes. J. Chem. Technol. Biotechnol. **81:**1601–1611.
21. **Grobler, J., F. Bauer, R. E. Subden, and H. J. J. van Vuuren.** 1995. The *mae1* gene of *Schizosaccharomyces pombe* encodes a permease for malate and other C_4 dicarboxylic acids. Yeast **11:**1485–1491.
22. **Güldener, U., S. Heck, T. Fiedler, J. Beinhauer, and J. H. Hegemann.** 1996. A new efficient gene disruption cassette for repeated use in budding yeast. Nucleic Acids Res. **24:**2519–2524.
23. **Haarasilta, S., and L. Taskinen.** 1977. Location of three key enzymes of gluconeogenesis in baker's yeast. Arch. Microbiol. **113:**159–161.
24. **Hohmann, S.** 1991. Characterization of *PDC6*, a third structural gene for pyruvate decarboxylase in *Saccharomyces cerevisiae*. J. Bacteriol. **173:**7963–7969.
25. **Inoue, H., H. Nojima, and H. Okayama.** 1990. High efficiency transformation of *Escherichia coli* with plasmids. Gene **96:**23–28.
26. **Kawagoe, M., K. Hyakumura, S. I. Suye, K. Miki, and K. Naoe.** 1997. Application of bubble column fermentors to submerged culture of *Schizophyllum commune* for production of L-malic acid. J. Ferment. Bioeng. **84:** 333–336.
27. **Kleijn, R. J., W. A. van Winden, W. M. van Gulik, and J. J. Heijnen.** 2005. Revisiting the ^{13}C-label distribution of the non-oxidative branch of the pentose phosphate pathway based upon kinetic and genetic evidence. FEBS J. **272:**4970–4982.
28. **Lange, H. C., and J. J. Heijnen.** 2001. Statistical reconciliation of the elemental and molecular biomass composition of *Saccharomyces cerevisiae*. Biotechnol. Bioeng. **75:**334–344.
29. **Lowry, O. H., N. J. Rosebrough, A. L. Farr, and R. J. Randall.** 1951. Protein measurement with the Folin phenol reagent. J. Biol. Chem. **193:**265–275.
30. **Lumyong, S., and F. Tomita.** 1993. L-Malic acid production by an albino strain of *Monascus araneosus*. World J. Microbiol. Biotechnol. **9:**383–384.
31. **Luttik, M. A. H., K. M. Overkamp, P. Kotter, S. de Vries, J. P. van Dijken, and J. T. Pronk.** 1998. The *Saccharomyces cerevisiae NDE1* and *NDE2* genes encode separate mitochondrial NADH dehydrogenases catalyzing the oxidation of cytosolic NADH. J. Biol. Chem. **273:**24529–24534.
32. **McAlister-Henn, L., J. S. Steffan, K. I. Minard, and S. L. Anderson.** 1995. Expression and function of a mislocalized form of peroxisomal malate dehydrogenase (MDH3) in yeast. J. Biol. Chem. **270:**21220–21225.
33. **Minard, K. I., and L. McAlister-Henn.** 1994. Glucose-induced phosphorylation of the Mdh2 isozyme of malate dehydrogenase in *Saccharomyces cerevisiae*. Arch. Biochem. Biophys. **315:**302–309.
34. **Minard, K. I., and L. McAlister-Henn.** 1991. Isolation, nucleotide sequence analysis, and disruption of the *MDH2* gene from *Saccharomyces cerevisiae*: evidence for three isozymes of yeast malate dehydrogenase. Mol. Cell. Biol. **11:**370–380.
35. **Minard, K. I., and L. McAlister-Henn.** 1992. Glucose-induced degradation of the Mdh2 isozyme of malate dehydrogenase in yeast. J. Biol. Chem. **267:**17458–17464.
36. **Mumberg, D., R. Müller, and M. Funk.** 1995. Yeast vectors for the controlled expression of heterologous proteins in different genetic backgrounds. Gene **156:**119–122.
37. **Ordiz, I., P. Herrero, R. Rodicio, and F. Moreno.** 1996. Glucose-induced inactivation of isocitrate lyase in *Saccharomyces cerevisiae* is mediated by the cAMP-dependent protein kinase catalytic subunits Tpk1 and Tpk2. FEBS Lett. **385:**43–46.
38. **Peleg, Y., A. Barak, M. C. Scrutton, and I. Goldberg.** 1989. Malic acid accumulation by *Aspergillus flavus*. III. ^{13}C NMR and isoenzyme analyses. Appl. Microbiol. Biotechnol. **30:**176–183.
39. **Peleg, Y., B. Stieglitz, and I. Goldberg.** 1988. Malic acid accumulation by *Aspergillus flavus*. I. Biochemical aspects of acid biosynthesis. Appl. Microbiol. Biotechnol. **28:**69–75.
40. **Pines, O., S. Even-Ram, N. Elnathan, E. Battat, O. Aharonov, D. Gibson, and I. Goldberg.** 1996. The cytosolic pathway of L-malic acid synthesis in *Saccharomyces cerevisiae*: the role of fumarase. Appl. Microbiol. Biotechnol. **46:**393–399.
41. **Pines, O., S. Shemesh, E. Battat, and I. Goldberg.** 1997. Overexpression of cytosolic malate dehydrogenase (MDH2) causes overproduction of specific organic acids in *Saccharomyces cerevisiae*. Appl. Microbiol. Biotechnol. **48:** 248–255.
42. **Postma, E., C. Verduyn, W. A. Scheffers, and J. P. Vandijken.** 1989. Enzymic analysis of the Crabtree effect in glucose-limited chemostat cultures of *Saccharomyces cerevisiae*. Appl. Environ. Microbiol. **55:**468–477.
43. **Rohde, M., F. Lim, and J. C. Wallace.** 1991. Electron microscopic localization of pyruvate carboxylase in rat liver and *Saccharomyces cerevisiae* by immunogold procedures. Arch. Biochem. Biophys. **290:**197–201.
44. **Sambrook, K., E. F. Fritsch, and T. Maniatis.** 1989. Molecular cloning: a laboratory manual. Cold Spring Harbor Laboratory Press, Cold Spring Harbor, NY.
45. **Schwartz, H., and F. Radler.** 1988. Formation of L(-)malate by *Saccharomyces cerevisiae* during fermentation. Appl. Microbiol. Biotechnol. **27:**553–560.
46. **Steffan, J. S., and L. McAlister-Henn.** 1992. Isolation and characterization of the yeast gene encoding the MDH3 isozyme of malate dehydrogenase. J. Biol. Chem. **267:**24708–24715.
47. **Stucka, R., S. Dequin, J. M. Salmon, and C. Gancedo.** 1991. DNA sequences in chromosomes II and VII code for pyruvate carboxylase isoenzymes in

Saccharomyces cerevisiae: analysis of pyruvate carboxylase-deficient strains. Mol. Gen. Genet. **229:**307–315.
48. **Taing, O., and K. Taing.** 2007. Production of malic and succinic acids by sugar-tolerant yeast *Zygosaccharomyces rouxii*. Eur. Food Res. Technol. **224:** 343–347.
49. **Takao, S., A. Yokota, and M. Tanida.** 1983. L-Malic acid fermentation by a mixed culture of *Rhizopus arrhizus* and *Paecilomyces varioti*. J. Ferment. Technol. **61:**643–645.
50. **van den Berg, M. A., P. De Jong-Gubbels, and H. Y. Steensma.** 1998. Transient mRNA responses in chemostat cultures as a method of defining putative regulatory elements: application to genes involved in *Saccharomyces cerevisiae* acetyl-coenzyme A metabolism. Yeast **14:**1089–1104.
51. **van Dijken, J. P., J. Bauer, L. Brambilla, P. Duboc, J. M. Francois, C. Gancedo, M. L. F. Giuseppin, J. J. Heijnen, M. Hoare, H. C. Lange, E. A. Madden, P. Niederberger, J. Nielsen, J. L. Parrou, T. Petit, D. Porro, M. Reuss, N. van Riel, M. Rizzi, H. Y. Steensma, C. T. Verrips, J. Vindeløv, and J. T. Pronk.** 2000. An interlaboratory comparison of physiological and genetic properties of four *Saccharomyces cerevisiae* strains. Enzyme Microb. Technol. **26:**706–714.
52. **van Maris, A. J., A., B. M. Bakker, M. Brandt, A. Boorsma, M. J. Teixeira de Mattos, L. A. Grivell, J. T. Pronk, and J. Blom.** 2001. Modulating the distribution of fluxes among respiration and fermentation by overexpression of *HAP4* in *Saccharomyces cerevisiae*. FEMS Yeast Res. **1:**139–149.
53. **van Maris, A. J. A., J. M. A. Geertman, A. Vermeulen, M. K. Groothuizen, A. A. Winkler, M. D. W. Piper, J. P. van Dijken, and J. T. Pronk.** 2004. Directed evolution of pyruvate decarboxylase-negative *Saccharomyces cerevisiae*, yielding a C_2-independent, glucose-tolerant, and pyruvate-hyperproducing yeast. Appl. Environ. Microbiol. **70:**159–166.
54. **van Urk, H., D. Schipper, G. J. Breedveld, P. R. Mak, W. A. Scheffers, and J. P. van Dijken.** 1989. Localization and kinetics of pyruvate-metabolizing enzymes in relation to aerobic alcoholic fermentation in *Saccharomyces cerevisiae* CBS 8066 and *Candida utilis* CBS 621. Biochim. Biophys. Acta **992:**78–86.
55. **van Winden, W. A., J. C. van Dam, C. Ras, R. J. Kleijn, J. L. Vinke, W. M. van Gulik, and J. J. Heijnen.** 2005. Metabolic-flux analysis of *Saccharomyces cerevisiae* CEN.PK113-7D based on mass isotopomer measurements of ^{13}C-labeled primary metabolites. FEMS Yeast Res. **5:**559–568.
56. **Verduyn, C., E. Postma, W. A. Scheffers, and J. P. van Dijken.** 1992. Effect of benzoic acid on metabolic fluxes in yeasts: a continuous-culture study on the regulation of respiration and alcoholic fermentation. Yeast **8:**501–517.
57. **Verduyn, C., T. P. L. Zomerdijk, J. P. Van Dijken, and W. A. Scheffers.** 1984. Continuous measurement of ethanol production by aerobic yeast suspensions with an enzyme electrode. Appl. Microbiol. Biotechnol. **19:**181–185.
58. **Volschenk, H., H. J. J. van Vuuren, and M. Viljoen-Bloom.** 2003. Malo-ethanolic fermentation in *Saccharomyces* and *Schizosaccharomyces*. Curr. Genet. **43:**379–391.
59. **Volschenk, H., M. Viljoen, J. Grobler, B. Petzold, F. Bauer, R. E. Subden, R. A. Young, A. Lonvaud, M. Denayrolles, and H. J. J. van Vuuren.** 1997. Engineering pathways for malate degradation in *Saccharomyces cerevisiae*. Nat. Biotechnol. **15:**253–257.
60. **Walker, M. E., D. L. Val, M. Rohde, R. J. Devenish, and J. C. Wallace.** 1991. Yeast pyruvate carboxylase: identification of two genes encoding isoenzymes. Biochem. Bioph. Res. Commun. **176:**1210–1217.
61. **Werpy, T., and G. Petersen (ed.).** 2004. Top value added chemicals from biomass, vol.I. Results of screening for potential candidates from sugars and synthesis gas. U.S. Department of Energy, Washington, DC. http://dx.doi.org/10.2172/15008859.
62. **Wiechert, W.** 2001. ^{13}C metabolic flux analysis. Metab. Eng. **3:**195–206.